NJC

ROYAL SOCIETY OF CHEMISTRY

PAPER

View Article Online
View Journal | View Issue

Cite this: *New J. Chem.*, 2020, **44**, 19759

Synthesis and antibacterial investigation of cationic waterborne polyurethane containing siloxane

Runping Jia, Zi Hui, Zhixiong Huang, Xin Liu, Cheng Zhao, Dayang Wang and Dandan Wu *

Received 16th September 2020,
Accepted 21st October 2020

DOI: 10.1039/d0nj04625f

rsc.li/njc

In this work, a cationic waterborne polyurethane (CWPU) dispersion containing siloxane in the side chain has been developed from 3-(2-aminoethylamino)propyldimethoxymethylsilane (APTS), using 3-dimethylamino-1,2-propanediol (DMAPD) as an ion centre. The DMAPD content was fixed constant and the effect of the APTS molar content on the particle size distribution and antibacterial performance of the CWPU dispersion, and hydrophobicity, water uptakes, crystallinity, thermal stability, surface morphology, of the forming CWPU films were wholly explored. The results indicated that more application of APTS into the CWPU might help strengthen the thermal stability and hydrophobicity for the cured films. What's more, as the molar content of APTS increased from 1% to 9%, all the CWPU dispersions reveal enhanced antibacterial activity against *Escherichia coli* and *Staphylococcus aureus*, and their maximum inhibition zone could reach 13.71 mm. This distinctly shows their great potential as antimicrobial coating materials. This work is the first in-depth study on the relationship between alkyl siloxane content and the antibacterial properties of cationic waterborne polyurethane dispersions and the resulting films.

1. Introduction

Polyurethane (PU) is a versatile polymeric material with molecular adaptability, excellent biocompatibility and mechanical properties, which is widely used in the fields of coatings, adhesives, medical equipment and packaging materials.[1–4] However, traditional polyurethane products contain organic solvents that generate volatile organic compounds (VOC) during use. With the increasing awareness of environmental protection, waterborne polyurethane materials have developed rapidly and become one of the most popular products.[5,6]

In actual use, waterborne polyurethane (WPU) will be interfered with by bacteria and microorganisms. Bacterial contamination on the surface of the material can lead to the formation of biofilms, pathogenic infections, damage to the surface of the material, and severe harm to health and even life.[7–9] Bacterial surface contamination has become a common problem, especially in the fields of healthcare, medical treatment, food storage, and water purification industries, where effective antibacterial WPUs are much desired. In order to block the interference of bacteria and microorganisms, various water polyurethane coatings containing release bactericide or contact bactericide have been developed, such as metal particles (Ag, Cu), nanocomposite particles (ZnO_2, SiO_2), organic quaternary ammonium salts (QAs), guanidine salt, *etc.*[10–13] QAs are one of the most proverbially applied antibacterial materials on contact surfaces due to their broad antibacterial spectrum and low bacterial resistance.[14,15] Recently, a few researchers have shown that the incorporation of hydrophobic fluorine components into antibacterial polymers can greatly enhance its antibacterial ability. Lin *et al.*[16] synthesized a series of cationic fluorinated acrylic emulsions and found that incorporating hydrophobic fluorine components into the polymer greatly improved the antibacterial activity. Zhao[17] *et al.* introduced fluorine-containing long alkyl chain quaternary salt compounds into the coating. However, due to the high toxicity and expensive cost of fluorine-containing compounds, their use has been dramatically limited. Siloxane has the dual advantages of inorganic and organic materials, which can enhance the thermal stability, water resistance, biocompatibility, and mechanical strength of WPU. Siloxane with non-polar characteristics tends to line up on the surface of the WPU film, provide low surface tension, and improve the hydrophobicity of the material.[18,19] There was little research on silicone-containing groups as chain extenders to prepare silicone-modified quaternary ammonium salt-type WPUs. In particular, few studies have been made regarding the influences of the alkoxy silane group on the antibacterial property of cationic waterborne polyurethane (CWPU).

School of Materials Science and Engineering, Shanghai Institute of Technology, Shanghai 201418, P. R. China. E-mail: wdan1008@163.com

Hence, on the basis of 3-dimethylamino-1,2-propanediol (DMAPD) as the hydrophilic ion centre of CWPU, 3-(2-aminoethylamino)propyldimethoxymethylsilane (APTS) as a diamine chain extender, a series of CWPUs with alkoxy siloxane groups was synthesized. The influence of the introduction of APTS on the particle size and antibacterial properties of the CWPU dispersion, hydrophobicity, water uptakes, crystallinity, thermal stability, and surface morphology of the CWPU films were mainly investigated. This work puts forward a practical and straightforward method to synthesize antibacterial CWPU.

2. Experimental

2.1. Materials

Isophorone diisocyanate (IPDI) and polybutylene adipate glycol (PBA, M_n = 2000) were obtained from BASF; 3-dimethylamino-1,2-propanediol (DMAPD) was obtained from Shanghai Titan. Dibutyltin dilaurate (DBTDL) catalyst, glacial acetic acid (Sigma), and 3-(2-aminoethylamino)-propyldimethoxymethylsilane (APTS) were purchased from Aladdin Reagent. To remove excess water, PBA was dehydrated under vacuum at 120 °C for 3 hours before use, and the other reagents were used directly. *Escherichia coli* (*E. coli*) and *Staphylococcus aureus* (*S. aureus*) were purchased from Guangdong Institute of Microbiology.

2.2. Preparation of CWPU dispersions

Based on PBA, IPDI, DMAPD and APTS, a series of cationic waterborne polyurethanes containing quaternary ammonium salts and siloxane have been synthesized, as shown in Fig. 1. First, PBA, which was dried under vacuum at 120 °C for 3 hours, was added to the three-necked flask. Under a dry nitrogen atmosphere, IPDI and DMAPD were added dropwise to the flask, which was reacted at 80 °C for 2 hours using DBTDL as a catalyst. The temperature was adjusted to 45 °C and subsequently, APTS was added to the above mixture with stirring for 1.5 hours. Then, acetic acid was charged into the flask as a

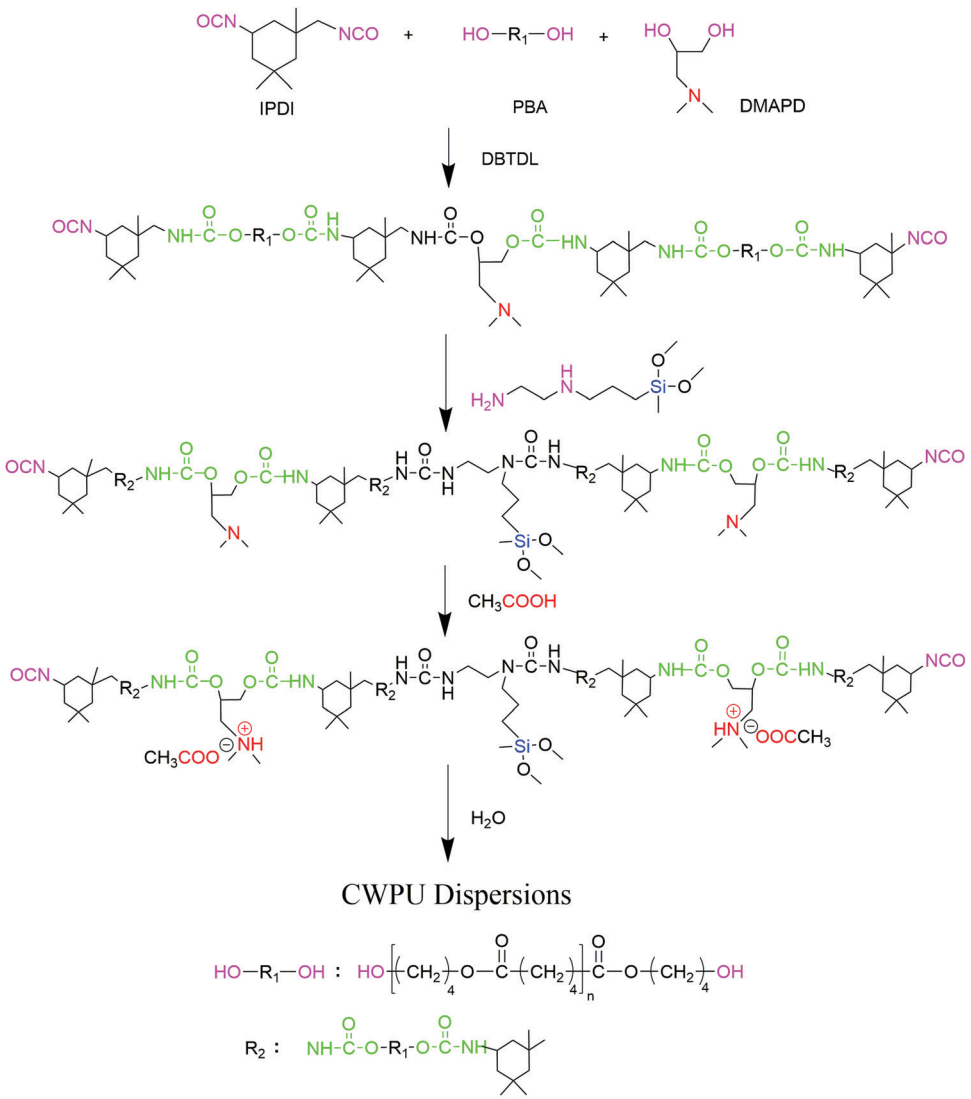

Fig. 1 Synthesis scheme of CWPU dispersions.

Table 1 Compositions of the CWPU

CWPU dispersion	IPDI (g)	PBA (g)	DMAPD (g)	APTS (g)	HAC (g)	H_2O (g)
CWPU0	8.892	27.170	2.714	0.000	1.368	116.327
CWPU1	8.892	26.400	2.660	0.158	1.340	114.329
CWPU3	8.892	24.880	2.576	0.473	1.298	110.461
CWPU5	8.892	23.356	2.487	0.788	1.253	106.567
CWPU7	8.892	21.831	2.395	1.103	1.207	102.662
CWPU9	8.892	20.305	2.304	1.418	1.161	98.757

neutralizer under room temperature stirring for 30 min. Finally, at a temperature of about 20 °C, by stirring at 900–1300 rpm for 45 min, the calculated amount of deionized water was added into the WPU prepolymer to obtain a dispersion. The samples were represented as CWPU0, CWPU1, CWPU3, CWPU5, CWPU7 and CWPU9, where the theoretical mole fractions of APTS in the total moles were 0, 1, 3, 5, 7 and 9% (Table 1).

2.3. Preparation of CWPU films

The CWPU film was prepared by casting the CWPU dispersion into a tetrafluoroethylene plate and then drying at 30 °C for about 96 h. The surface dry film was annealed in a vacuum oven at 60 °C for 12 hours, and finally stored in a desiccator at room temperature.

2.4. Characterization of WCPU

The FTIR spectra were obtained using a Nicolet iN10 (Thermo Fisher Scientific, USA) to analyse the CWPU membrane structure. The FTIR spectrum of the sample was recorded with a resolution of 4 cm^{-1} and 32 scans in the range of 4000–500 cm^{-1}.

The average particle size and zeta potential of the CWPU emulsion were tested by dynamic light scattering using the PALS Zeta potential and DLS nanometer particle size analyzer (Brookhaven Instruments, Inc.) at 25 °C. The tested emulsion was diluted to transparent or translucent, the number of scans was three, and the test results were averaged. The CWPU dispersion was centrifuged on TDL-40B at a rate of 3000 rpm for 30 minutes to evaluate the storage stability.

At room temperature, the static water contact angle (WCA) was measured using a water contact angle tester (OCA20, Hamburg, Germany).

In order to measure the water absorption of the films, CWPU films (1 cm × 1 cm) were immersed in deionized water at 25 °C for 168 h. After wiping the surface of the film with an absorbent filter paper to dry it, the water absorption of the swollen film was measured through the following formula:

$$\text{Absorption } (\%) = \frac{m_1 - m_0}{m_0} \times 100$$

where m_1 is the weight of the film after absorbing water and m_0 is the weight of the film before water absorption.

The crystallinity of the CWPU sample was obtained by wide-angle X-ray diffraction (XRD). The scanning range of 2θ angle of the CWPU film is from 5 to 60°.

The thermal weight loss of the CWPU films was measured using a STA449F3 thermal gravimetric analyzer (TGA) between 25 °C and 600 °C.

The thermal properties of CWPU film samples were performed by differential scanning calorimetry (DSC).

In order to evaluate the microscopic morphology of the surface of the CWPU film, scanning electron microscopy (SEM, JSM-7001F, JPN) was used at an accelerating voltage of 25 kV.

Antibacterial studies. The disc diffusion method was used to determine the antibacterial ability of the obtained CWPU toward *Escherichia coli* and *Staphylococcus aureus*. Briefly, the cell suspension (approximately 10^8 CFU mL^{-1}) was evenly spread on Mueller–Hinton agar. A paper disc with a diameter of 6 mm was attached to the Mueller–Hinton agar, and then the CWPU dispersion (20 μg) was added to the paper disc. After the M–H agar plate was incubated at 37 °C, the area of inhibition was measured using a precision caliper. After incubating the M–H agar plate for one day at 37 °C, the diameter of the inhibition zone was measured using a precision caliper. To further verify the antibacterial type of the CWPU membrane, an inhibition zone test was used to investigate whether there is active QA material leached from the film.

3. Results and discussion

3.1. Characterization of the CWPU structure

In this study, FTIR technology was used to analyse the chemical structure of CWPU0, CWPU1, CWPU3, CWPU5, CWPU7 and CWPU9 membranes. The ATR-FTIR results are shown in Fig. 2, and the ATR-FTIR spectra of all samples are very similar. According to the figure, the disappearance of 2270 cm^{-1} (N═C═O tensile vibration) shows that all isocyanate was exhausted, which indicates that DMAPD and PBA have completely reacted with excess IPDI. Peaks at 800 cm^{-1} and 1160 cm^{-1} are assigned to the stretching vibrations of Si–O–Si.[20] The appearance and enhancement of the characteristic peak at 800 cm^{-1} indicate that a crosslinked network can be generated by the hydrolysis and condensation reaction of the siloxane group from APTS. The absorption peak around 3000–3400 cm^{-1} belongs to N–H vibration in urethane, urea bond and quaternary ammonium salt. The stretching vibration peak of C–H appears

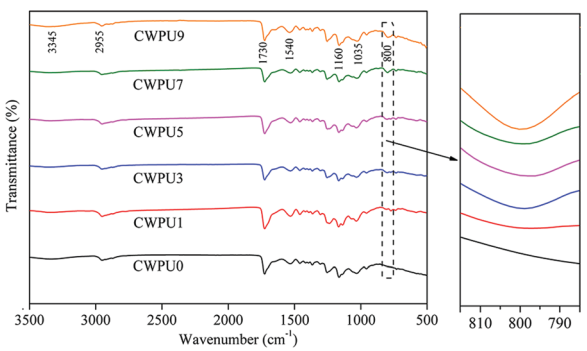

Fig. 2 Infrared spectra of different CWPU membranes.

at 2890–2990 cm^{-1}, and the peak at 1730 cm^{-1} is assigned to the stretching vibration of the carbonyl group (C═O) in the carbamate (–NHCOO–). The peak near 1035 cm^{-1} is the comprehensive performance of C–O–C stretching vibration and Si–O–Si asymmetric stretching vibration.[21] As the content of APTS increases, it can be further observed that C═O at 1730 cm^{-1} also gradually weakens, which may be caused by the change in hydrogen bonding of the system.[22] These preliminarily have proved the successful preparation of CWPU emulsion containing silicone.

3.2. Dispersibility of CWPU emulsion

In this study, the laser particle size analyzer was used to measure the average particle size of the CWPU dispersion. In Fig. 3, the prepared CWPU dispersions show a homogeneous particle size distribution observing that the CWPU prepolymer containing DMAPD can be distributed in water to obtain a steady aqueous polyurethane dispersion. The minimum particle size of CWPU emulsion was 34.9 nm. As the amount of APTS increased, the average particle size of the CWPU dispersion continued to grow. When the amount of APTS was more significant than 3%, the increase in particle size was particularly significant, from 57.2 nm to 140.9 nm. The rise of particle size is typical in siloxane-modified WPU systems, which is related to the increasing incompatibility of the system and the partial hydrolysis and cross-linking of siloxane in water.[23] On the other hand, APTS as a chain extender, with its amount increasing the degree of cross-linking between molecules and the molecular weight increase, which limits the movement of the molecular chain. The increase in molecular weight may cause the entanglement of CWPU chains and result in a larger particle size. The appearance of a series of synthesized CWPU dispersions with different APTS concentrations is also shown in Fig. 3. As the particle size increases, it can be seen that the dispersion exhibits different colours, and the dispersion changes from transparent to milky white. As determined by DLS, the zeta potential of quaternary ammonium salt type waterborne polyurethane emulsion is 60.3 mV to 30.0 mV (Table 2). Besides, there is no distinct stratification or precipitation of the

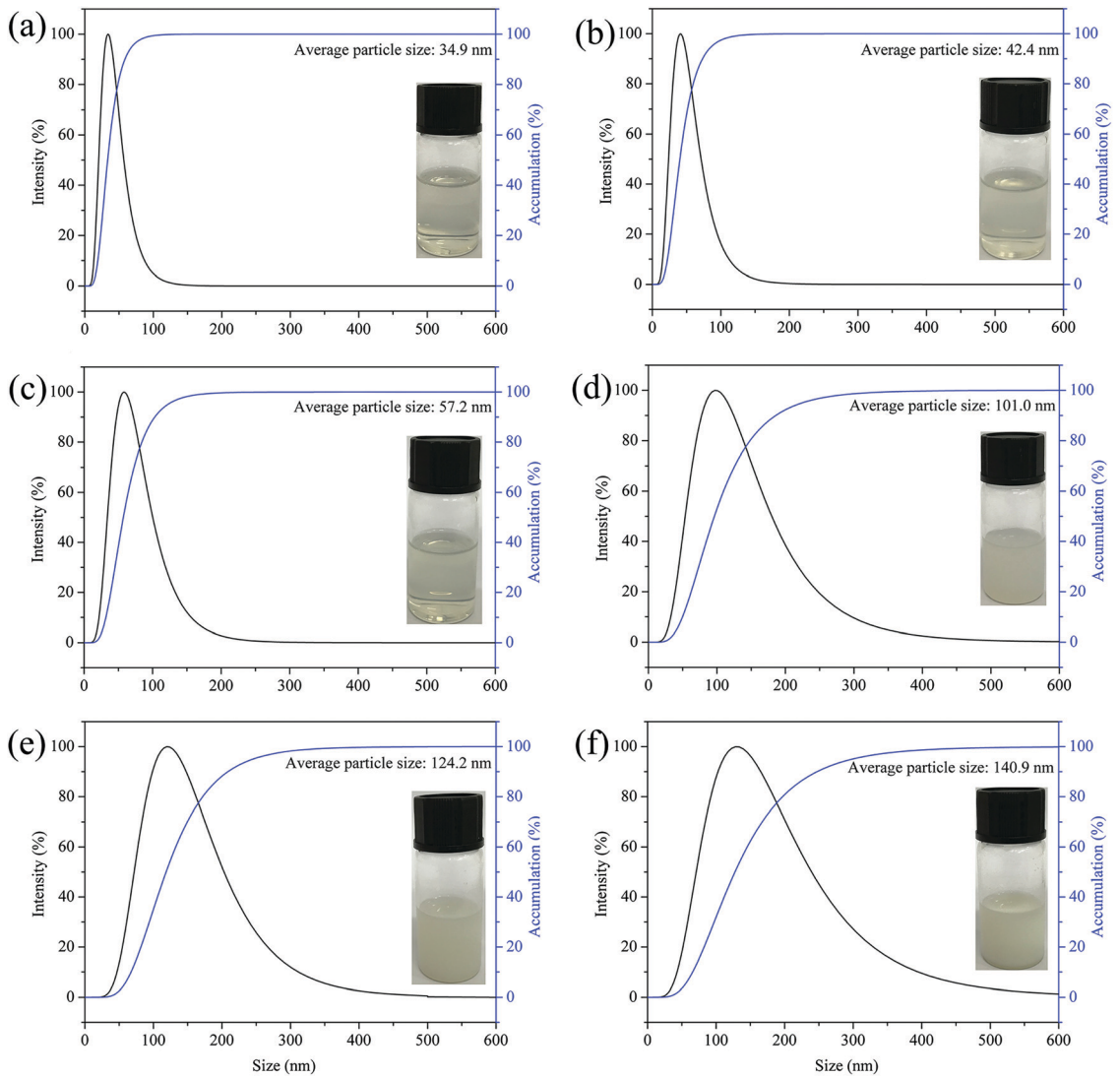

Fig. 3 Particle size curves of CWPU dispersions, (a) CWPU0; (b) CWPU1; (c) CWPU3; (d) GWFPU4; (e) CWPU7; (f) CWPU9.

Table 2 Zeta potential of different CWPUs

Samples	CWPU0	CWPU1	CWPU3	CWPU5	CWPU7	CWPU9
Zeta potential (mV)	57.5	60.3	61.5	56.0	48.2	30.0

CWPUs after centrifugation. These results demonstrate that the CWPU dispersions prepared with different APTS contents have excellent storage stability.

3.3. The WCA and water adsorption of CWPU membranes

Static WAC test can be used to study the surface hydrophobic properties of materials. The WCA data of the prepared CWPU film is shown in Fig. 4. The results show that the WCA values of the prepared films were 68.5° (CWPU0), 79.2° (CWPU1), 88.0° (CWPU3), 91.2° (CWPU5), 95.6° (CWPU7), and 104.9° (CWPU9), indicating that the hydrophobicity of the CWPU film greatly increases with the content of APTS because of the hydrophobic organosiloxane.[24] In the process of film formation, the presence of low-polarity siloxane can provide a driving force to migrate to the surface of the polyurethane film and lead to the surface being more hydrophobic, thus making the WCA values increase.[25,26] In this study, the surface hydrophobicity of the WPU film was evidently higher than previously reported.[21]

With the improvement of surface hydrophobicity, the water absorption rate of the CWPU film would be significantly reduced. As given in Fig. 5, the film CWPU0 without APTS has a water absorption rate of 20% within 24 hours. The test curve shows that the water absorption rate of CWPU1 and CWPU3 samples are higher than 10% within 48 hours. It can be seen from the curves of CWPU3 and CWPU5 that the water absorption rate drops to 10% within 24 hours, and then slightly increases from 48 hours to 168 hours. The water absorption rate of CWPU7 and CWPU9 dropped to about 8% and reached equilibrium within 72 hours. What's more, the sample with the minimum water absorption rate is CWPU9 due to its high content of siloxane. In contrast to the CWPU0 sample, the introduction of APTS into the polyurethane skeleton (CWPU1–CWPU9) could deeply decrease the water absorption. This phenomenon could be attributed to the establishment of hydrophobic surface and

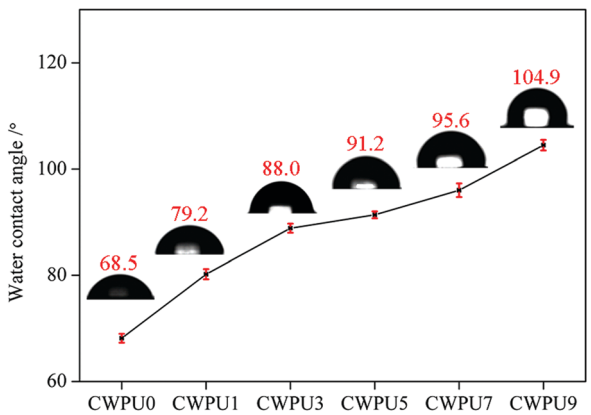

Fig. 4 WCA value of CWPU films.

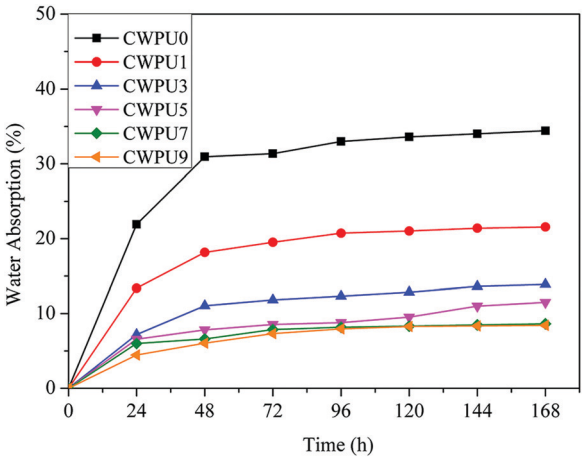

Fig. 5 Water absorption of CWPU films.

crosslinked structures. Besides the surface hydrophobicity which can make the membrane block water, the cross-linked network structure formed by Si–O–Si in the system can build a highly cross-linked film matrix and effectively reduce the water absorption.

3.4. XRD analysis

In CWPU, the crystal formation is mainly affected by the hydrogen bond between the hard segment and the soft segment. The crystal structures of the prepared polymers CWPU0, CWPU1, CWPU3, CWPU5, CWPU7 and CWPU9 were measured by wide-angle X-ray diffraction (Fig. 6). The diffuse diffraction peak at 2θ = 21.5°, characteristic of the soft segments in WPU, demonstrates that there were crystalline regions in the internal structure of these films.[27] This result may be due to the presence of PBA in the CWPU film. In addition, the XRD pattern shows that there are some crystallites in the system. The peak intensity around 21.5° lessens with the increase of APTS content, which indicates that the crystallinity of CWPU membranes progressively weakened. Fig. 6(b) shows that the calculated crystallization of CWPU films were 21.8% (CWPU0), 20.1% (CWPU1), 17.7% (CWPU3), 13.0% (CWPU5), 9.7% (CWPU7), and 6.5% (CWPU9). This phenomenon may result from the formation of a Si–O–Si cross-linked structure, which limits the movement and orderly arrangement of the chain segments and reduces the regularity of the soft segments. Eventually, the regular arrangement at some parts in these CWPU films was destroyed.[28]

3.5. Thermal properties of the CWPU films

Fig. 7(a) displays the relationship between APTS content and the thermal stability of different CWPU composite membranes. The weight loss under 250 °C may result from the volatilization of residual water and organic solvent in the CWPU membranes. The primary weight loss process of the CWPU film occurs above 250 °C, which is divided into two stages, namely, the thermal decomposition of hard and soft segments. The partial decomposition of the hard segment occurs in the range of 250 °C to

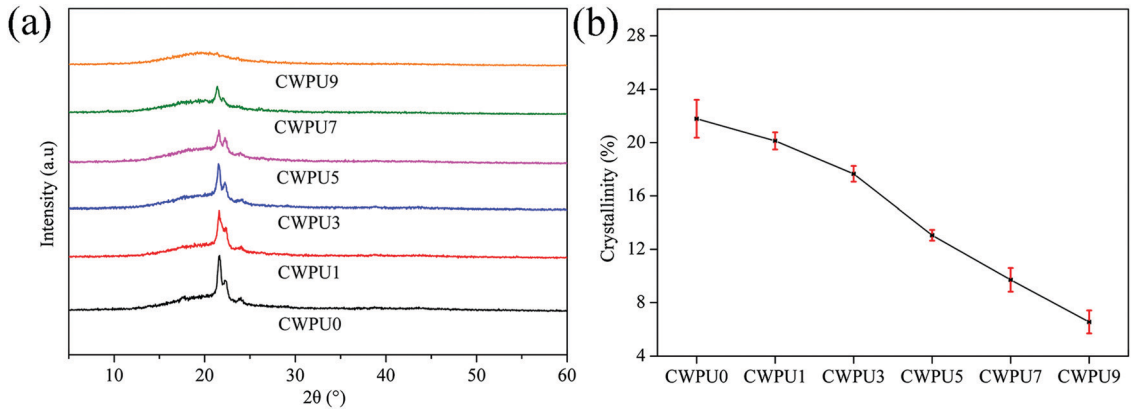

Fig. 6 XRD spectra (a) and crystallinity (b) of CWPU membranes.

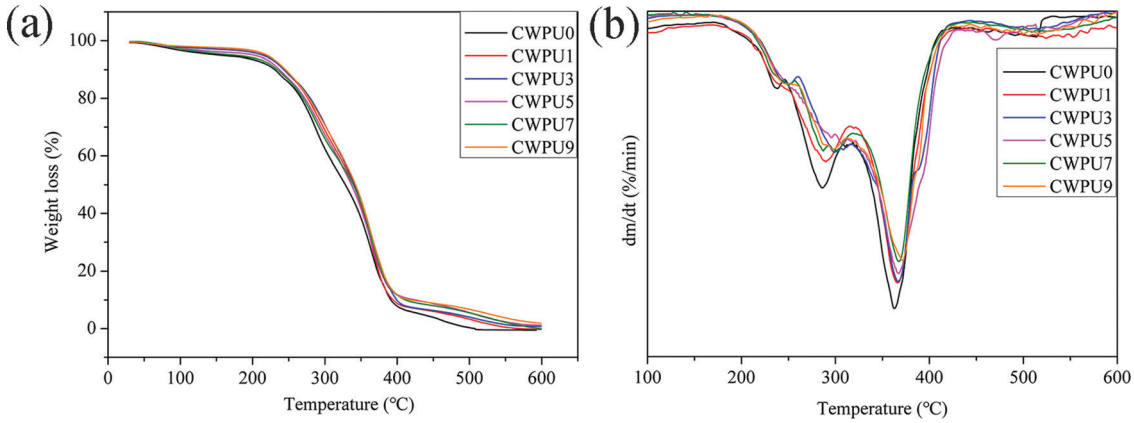

Fig. 7 TG curves (a) and DTG curves (b) of CWPU films.

360 °C, which can be demonstrated by the rapid weight loss of isocyanate, urea and amine. The weight loss in the range of 360 °C to 450 °C is primarily the decomposition of polyester in the soft segment.[29] The decomposition above 450 °C is mainly due to the fracture of the cross-linked structure in the CWPU film. Finally, the main dissolution product of thermal weight loss is SiO_2.

Fig. 7(b) shows the thermal weight loss rate of different CWPU membranes between 100 °C and 600 °C. There are two maximum thermal weight loss rates T_{max1} and T_{max2}. As the molar content of APTS increases from 0% to 9%, the T_{max1} increased from 285 to 302 °C, and the T_{max2} increased from 362 to 375 °C. The improved thermal stability of the CWPU film can be attributed to the strong bond energy of Si–O (460 kJ mol^{-1}). Moreover, the presence of APTS can form a Si–O–Si crosslinked network, which can enhance the interaction between molecular chains and strengthen the thermal stability of CWPU.[30]

3.6. DSC analysis of the CWPU films

Differential scanning calorimeter (DSC) was used to study the thermal transition behaviours of CWPU0, CWPU1, CWPU3, CWPU5, CWPU7 and CWPU9 polymers. The glass transition temperature (T_g) of each sample was observed in Fig. 8. Compared to CWPU0, the T_g values of CWPU1, CWPU3, CWPU5, CWPU7, and CWPU9 containing APTS slightly ascended. This phenomenon resulted from the introduction of APTS increased cross-link density and rigid structure, which reduced polymer

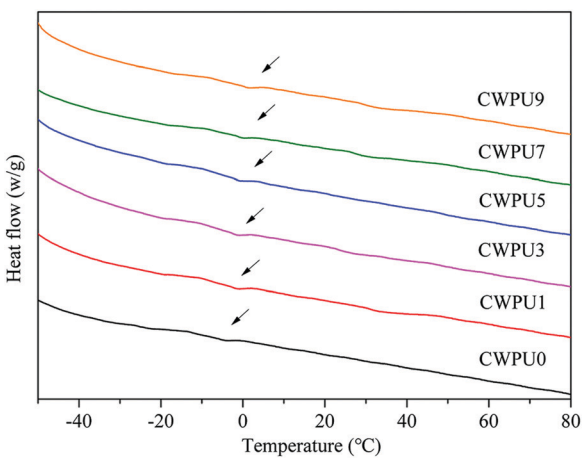

Fig. 8 DSC curves of CWPU films with different APTS contents.

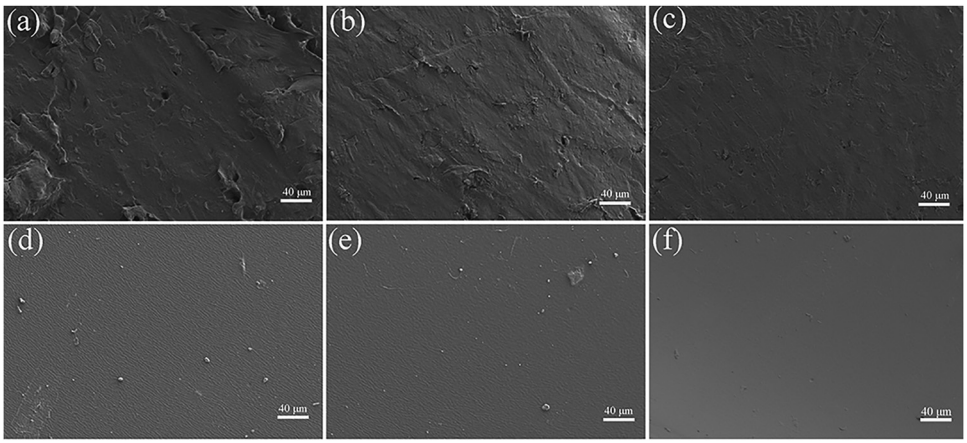

Fig. 9 SEM images of the surfaces of the CWPU films, (a) CWPU0; (b) CWPU1; (c) CWPU3; (d) GWFPU4; (e) CWPU7; (f) CWPU9.

chain movement.[31–33] When the content of APTS was 0, 1, 3, 5, 7 and 9 mol%, the T_g values of the CWPU films were −2.7 °C, −1.6 °C, −0.7 °C, −0.3 °C, 1.4 °C and 2.5 °C, respectively.

3.7. Surface morphology of the CWPU film

Fig. 9 shows the surface morphologies of the WPU films characterized by SEM. The surface of CWPU0, CWPU1 and CWPU3 films were relatively rough, with some protrusions in the whole region, and the protrusions on the surface gradually decreased as the amount of APTS increases. When the molar amount of APTS was more significant than 3%, the surface of the CWPU film gradually became smooth and flat, which can be evidenced by microphotographs of CWPU5, CWPU7 and CWPU9. The surface of CWPU7 and CWPU9 films was very smooth and significantly differed from the films containing lower APTS content. It is known that for block-type WPU copolymer, its chemical composition, molecular chain length, and content of hard segments and soft segments involve a significant part in the formation of phase-separated microstructures.[34] In this study, polyester polyols and Si–O–Si moieties were the soft segments of polyurethane and urethane and urea groups were assigned to the hard segment of CWPU. Due to the low surface energy of the inorganic Si–O bond in siloxane, the silane part migrates to the film surface.[35] With the increase of APTS content, the microphase separation between the hard and soft segments of CWPU becomes more serious, and its surface is completely encapsulated by siloxane.[36] The siloxane part enriches the surface of the CWPU film, making the SEM image smoother.

3.8. The antibacterial activity of CWPU

Generally, polymeric substances with quaternary ammonium groups have been extensively studied and used in antibacterial-relevant applications.[37,38] It is known that quaternary ammonium groups with a positive charge can attract the bacterial cells which are negatively charged.[39] Recent studies on the mechanism of contact sterilization suggest that the specific adsorption of negatively charged phospholipids onto the cationic, hydrophobic surface and interference with membrane potential could result in a strong shape deformation of bacterial cells.[40] The consequences will lead to irreparable membrane damage and cell death. Organosiloxane is a superior material that can impart excellent biocompatibility, hydrophobicity and antibacterial properties to the polyurethane material.[41,42] Hence, in this study, the content of DMAPD is fixed, the APTS content, which provides siloxane groups, may play a major role in terms of the antibacterial performance of the CWPU.

Table 3 and Fig. 10 exhibit the antibacterial activity of the CWPU. Apparent inhibition zones can be observed demonstrating that CWPU emulsions containing the QAs group display excellent bactericidal activity against *E. coli*. CWPU7 and CWPU9 show the best antibacterial activity among the CWPUs due to their highest APTS content indicating that the rise of siloxane groups improves the antibacterial activity of the CWPUs. This phenomenon may result from the siloxane group, which can enhance the compatibility and hydrophobicity of CWPU emulsion. The sample containing siloxanes are more likely to spread through the bacterial wall and disrupt the plasma membrane, leading to the death of the bacteria.[43–45] CWPU9 (zone of inhibition is 12.01 mm) with the highest APTS content shows slightly lower antibacterial activity than CWPU7 (zone of inhibition is 13.62 mm). This phenomenon may be due to the highest APTS content of CWPU9. The increase in siloxane content increases the cross-linked density of the resulting polymer, resulting in reduced pervasion of CWPU9 than the CWPU7. Hence, CWPU7 exhibits more effective physical interaction with

Table 3 Zone of inhibition of the CWPUs

Samples	Inhibition zones of CWPUs against *Escherichia coli* (mm)	Inhibition zones of CWPUs against *Staphylococcus aureus* (mm)
CWPU0	9.81	9.89
CWPU1	10.02	11.75
CWPU3	10.30	12.06
CWPU5	11.50	12.55
CWPU7	13.62	13.71
CWPU9	12.01	12.80

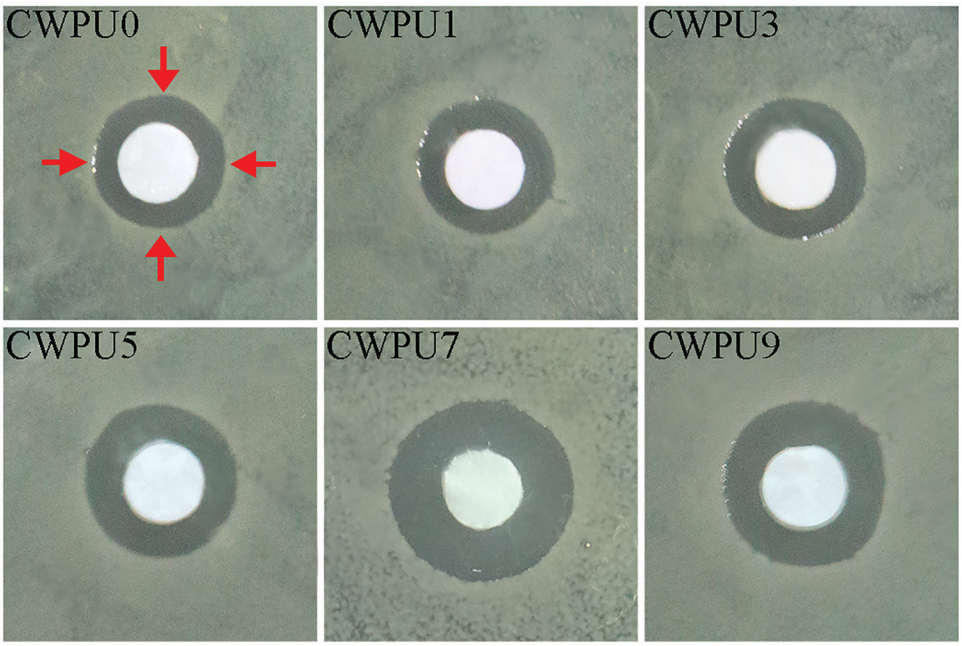

Fig. 10 The antibacterial activities of the CWPUs against *Escherichia coli*.

target bacteria than CWPU9 and has better antibacterial activity. In addition, Fig. 11 shows the antibacterial activity of the resulting CWPUs against *Staphylococcus aureus*. The prepared samples display higher antimicrobial activity against *S. aureus*, which may be due to the different composition and structure of the microorganisms.[46,47] In general, all the prepared CWPUs exhibit excellent bactericidal performance, revealing their great potential as antimicrobial coating materials.

To determine the antibacterial type of the CWPU material, Fig. 12 shows the antibacterial properties of the CWPU film. An inhibition zone could not be discovered around the CWPU7 film, which confirms that there are no antibacterial substances released.[48] The schematic diagram of the antibacterial process is shown in Fig. 12(c) to further investigate the antibacterial mechanism of the CWPU film. It is known that the surface of APTS-containing samples becomes smoother, more hydrophobic

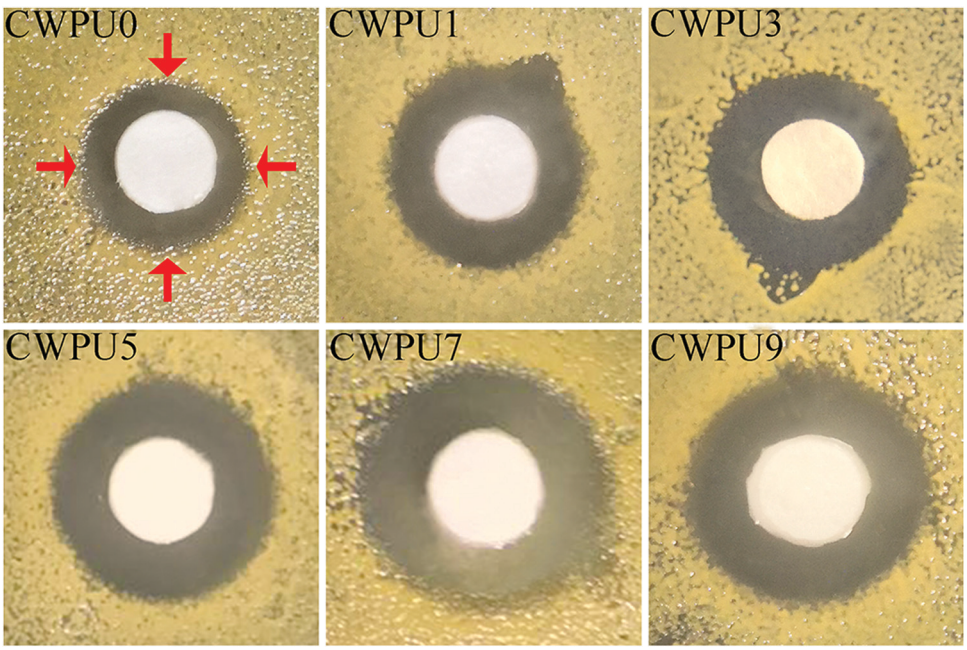

Fig. 11 The antibacterial activities of CWPUs against *Staphylococcus aureus*.

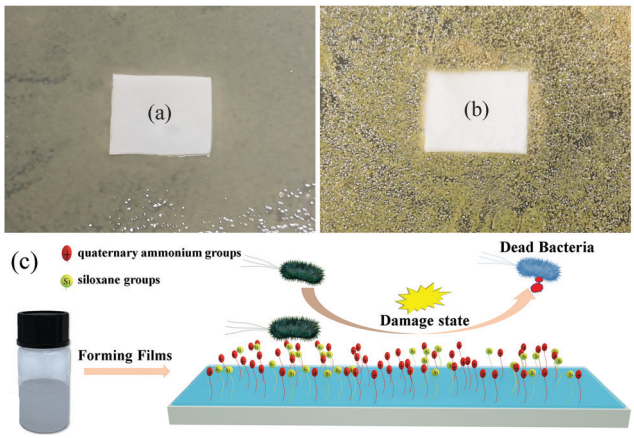

Fig. 12 (a) and (b) Show the text results of the CWPU7 membrane in *E. coli* and *Staphylococcus aureus*. (c) Shows the process of the antibacterial CWPU film.

and has low surface energy because of siloxane. These properties make the CWPU membrane containing QAs harder to be contaminated by microorganisms. The initial contact was through electrostatic interaction (negatively charged bacteria and positively charged QAs) and hydrophobic interaction (the alkyl and siloxanes groups with membrane proteins of bacteria). Then, the bacterial structure was destroyed (the destruction of the cytoplasmic membrane and the leakage of cytoplasmic components). It can be inferred that the polymer chains may interact more effectively with the bacteria due to its nearby siloxane component causing the enhancement of cell compatibility to promote deeper penetration of the polymer chain inside the bacteria which disrupts the cytoplasmic constituents. The destruction of cell structure eventually leads to cell death.

4. Conclusions

In this work, antibacterial CWPU dispersions containing siloxane in the side chains were developed. As the APTS content increases, the average particle size of these CWPUs ranges from 34.9 nm to 140.9 nm. All these samples exhibit good storage stability, and there was no obvious stratification when the CWPUs were stored for 12 months at room temperature. The performances of the synthetic CWPU films demonstrated that the incorporation of APTS into CWPUs could improve thermal resistance, water repellency and surface morphology. In particular, the water contact angle of these novel CWPU films increased from 68.5° to 104.9°, which allows the resulting CWPU to be more widely used in the coating industry. What's more, all the CWPU samples showed excellent antibacterial activity, particularly against *Staphylococcus aureus*, revealing their enormous potential as antimicrobial coating materials in the application of medical instruments and food processing.

Conflicts of interest

There are no conflicts of interest.

Acknowledgements

The research was financially supported by the National Science Youth Foundation (21106083), the Natural Science Foundation of Shanghai (19ZR1455000), the Shanghai Engineering Research Center of Building Waterproof Materials (18DZ2253200), and the Shanghai Alliance Program (LM201933, LM201951).

References

1 M. Joshi, B. Adak and B. S. Butola, *Prog. Mater. Sci.*, 2018, **97**, 230–282.
2 L. Xiao, M. Deng, W. Zeng, B. Zhang, Z. Xu, C. Yi and G. Liao, *Ind. Eng. Chem. Res.*, 2017, **56**, 12354–12361.
3 P. Yang, Y. Wang, L. Lu, X. Yu and L. Liu, *Appl. Surf. Sci.*, 2018, **435**, 346–351.
4 P. Król and B. Król, *J. Mater. Sci.*, 2020, **55**, 73–87.
5 S. Mehravar, N. Ballard, R. Tomovska and J. M. Asua, *Ind. Eng. Chem. Res.*, 2019, **58**, 20902–20922.
6 Q. Liu, B. Liao, H. Pang, M. Lu and Y. Meng, *Prog. Org. Coat.*, 2020, **143**, 105551.
7 M. S. Ganewatta and C. Tang, *Polymer*, 2015, **63**, A1–A29.
8 J. Liu, X. Chen, H.-y. Shu, X.-r. Lin, Q.-x. Zhou, T. Bramryd, W.-s. Shu and L.-n. Huang, *Environ. Pollut.*, 2018, **235**, 171–179.
9 K. Burugapalli, S. Wijesuriya, N. Wang and W. Song, *J. Biomed. Mater. Res., Part A*, 2018, **106**, 1072–1081.
10 L. Valenzuela, A. Iglesias-Juez, B. Bachiller-Baeza, M. Faraldos, A. Bahamonde and R. Rosal, *J. Mater. Chem. B*, 2020, **8**, 8294–8304.
11 V. Rajendran, N. R. Dhineshbabu, R. R. Kanna and K. V. I. S. Kaler, *Ind. Eng. Chem. Res.*, 2014, **53**, 19512–19524.
12 B. Zhao, R. Jia, Y. Zhang, D. Liu and X. Zheng, *J. Appl. Polym. Sci.*, 2019, **136**, 46923.
13 S. Du, Y. Wang, C. Zhang, X. Deng, X. Luo, Y. Fu and Y. Liu, *J. Mater. Sci.*, 2018, **53**, 215–229.
14 W. He, Y. Zhang, F. Luo, J. Li, K. Wang, H. Tan and Q. Fu, *RSC Adv.*, 2015, **5**, 89763–89770.
15 Y. Zhang, X. He, M. Ding, W. He, J. Li, J. Li and H. Tan, *Biomacromolecules*, 2018, **19**, 279–287.
16 J. Lin, X. Chen, C. Chen, J. Hu, C. Zhou, X. Cai, W. Wang, C. Zheng, P. Zhang, J. Cheng, Z. Guo and H. Liu, *ACS Appl. Mater. Interfaces*, 2018, **10**, 6124–6136.
17 J. Zhao, W. Millians, S. Tang, T. Wu, L. Zhu and W. Ming, *ACS Appl. Mater. Interfaces*, 2015, **7**, 18467–18472.
18 Z. Cheng, Q. Li, Z. Yan, G. Liao, B. Zhang, Y. Yu, C. Yi and Z. Xu, *Prog. Org. Coat.*, 2019, **127**, 194–201.
19 Y. Xia and R. Larock, *Macromol. Rapid Commun.*, 2011, **32**, 1331–1337.
20 Q. Li, J. Ye, T. Qiu, L. Guo, L. He and X. Li, *J. Appl. Polym. Sci.*, 2018, **135**, 46628.
21 J. Lyu, K. Xu, N. Zhang, C.-S. Lu, Q. Zhang, L. Yu, F. Feng and X. Li, *Molecules*, 2019, **24**, 1667.
22 H. Zhou, H. Wang, X. Tian, K. Zheng and Q. Cheng, *Prog. Org. Coat.*, 2014, **77**, 1073–1078.

23 Q. Zhang, J. Hu and S. Gong, *J. Appl. Polym. Sci.*, 2011, **122**(5), 3064–3070.
24 S. Xu, L. Xie, X. Yu, Y. Xiong and H. Tang, *J. Polym. Sci., Part A: Polym. Chem.*, 2015, **53**, 1794–1805.
25 G. Wu, D. Liu, J. Chen, G. Liu and Z. Kong, *Prog. Org. Coat.*, 2019, **127**, 80–87.
26 X. Zhao, Y. Li, B. Li, T. Hu, Y. Yang, L. Li and J. Zhang, *J. Colloid Interface Sci.*, 2019, **542**, 8–14.
27 L. Lei, Y. Zhang, C. Ou, Z. Xia and L. Zhong, *Prog. Org. Coat.*, 2016, **92**, 85–94.
28 L. Lei, L. Zhong, X. Lin, Y. Li and Z. Xia, *Chem. Eng. J.*, 2014, **253**, 518–525.
29 Z. Petrović, L. Yang, A. Zlatanic, W. Zhang and I. Javni, *J. Appl. Polym. Sci.*, 2007, **105**, 2717–2727.
30 D. K. Chattopadhyay and D. C. Webster, *Prog. Polym. Sci.*, 2009, **34**, 1068–1133.
31 Q. Li, J. Li, G. Liao and Z. Xu, *J. Mater. Sci.: Mater. Med.*, 2018, **29**, 126.
32 E. Sun, G. Liao, Q. Zhang, P. Qu, G. Wu, Y. Xu, C. Yong and H. Huang, *Materials*, 2018, **11**, 1695.
33 K. M. Seeni Meera, R. Murali Sankar, S. N. Jaisankar and A. B. Mandal, *J. Phys. Chem. B*, 2013, **117**, 2682–2694.
34 M. V. Pergal, J. V. Džunuzović, R. Poręba, S. Ostojić, A. Radulović and M. Špírková, *Prog. Org. Coat.*, 2013, **76**, 743–756.
35 H. Zhao, D. Huang, H. Tonghui, G.-H. Hu, G.-b. Ye, T. Jiang and Q.-C. Zhang, *New J. Chem.*, 2017, **41**, 9268–9275.
36 H. Zhao, W. She, D. Shi, W. Wu, Q.-c. Zhang and R. K. Y. Li, *Composites, Part B*, 2019, **177**, 107441.
37 J. Wu, C. Wang, C. Mu and W. Lin, *Eur. Polym. J.*, 2018, **108**, 498–506.
38 Y. Zhang, Y. Li, J. Li, Y. Gao, H. Tan, K. Wang, J. Li and Q. Fu, *Sci. Bull.*, 2015, **60**, 1114–1121.
39 A. Muñoz-Bonilla and M. Fernández-García, *Prog. Polym. Sci.*, 2012, **37**, 281–339.
40 N. Rauner, C. Mueller, S. Ring, S. Boehle, A. Strassburg, C. Schoeneweiss, M. Wasner and J. Tiller, *Adv. Funct. Mater.*, 2018, **28**, 1801248.
41 S. Park, J.-Y. Kim, W. Choi, M.-J. Lee, J. Heo, D. Choi, S. Jung, J. Kwon, S.-H. Choi and J. Hong, *Chem. Eng. J.*, 2020, **393**, 124686.
42 J. Jiang, Y. Fu, Q. Zhang, X. Zhan and F. Chen, *Appl. Surf. Sci.*, 2017, **412**, 1–9.
43 H.-Y. Lee, H.-E. Kim and S.-H. Jeong, *Colloids Surf., B*, 2019, **174**, 308–315.
44 T. Tashiro, *Macromol. Mater. Eng.*, 2001, **286**, 63–87.
45 G. Cheng, H. Xue, Z. Zhang, S. Chen and S. Jiang, *Angew. Chem., Int. Ed.*, 2008, **47**, 8831–8834.
46 L. M. Timofeeva, N. A. Kleshcheva, A. F. Moroz and L. V. Didenko, *Biomacromolecules*, 2009, **10**, 2976–2986.
47 L. Man, Y. Feng, Y. Hu, T. Yuan and Z. Yang, *J. Cleaner Prod.*, 2019, **241**, 118341.
48 Y. Wang, R. Chen, T. Li, P. Ma, H. Zhang, M. Du, M. Chen and W. Dong, *Ind. Eng. Chem. Res.*, 2020, **59**, 458–463.

